Investigation of the Aerosol Indirect Effect During the Atmospheric Radiation Measurement Program's March 2003 Aerosol Intensive Operational Period at the Southern Great Plains: Sensitivity Tests

H. Guo and JE Penner
Department of Atmospheric, Oceanic, and Space Sciences
University of Michigan
Ann Arbor, Michigan

Introduction

Clouds and their related physical processes present perhaps the most complicated and perplexing problems in the study of climate change and weather forecasting (Stephens 2005). One important cloud-related process is the aerosol-cloud-radiation interaction, or the so-called aerosol indirect effect (AIE). The AIE is estimated to vary from 0.0 to -4.8 W/m^2 in state-of-the-art global climate models (Penner et al. 2001). The uncertainty in this estimation has stimulated substantial research in recent years. Most of this research focuses on the first AIE, the second AIE, or both.

The first AIE mainly refers to the modification of the cloud droplet number concentration (N_d) by aerosols, which is also called "Twomey" effect. Twomey (1977) showed that a higher aerosol number concentration (N_a) would result in a higher N_d and a smaller mean droplet size, and thereby lead to a higher cloud reflectivity if the cloud water content kept unchanged. The first AIE is widely supported by a variety of measurements (e.g., in situ airborne measurements and ground-based remote sensing). By analyzing the airborn measurement during the Second Aerosol Characterization Experiment, Brenguier et al. (2000) showed that N_d could characterize the contamination of the air mass, and that the difference of cloud radiative properties between polluted and clean cases was noticeable. Using ground-based remote sensing data, Penner et al. (2004) showed that the cloud optical depth differed in clean and polluted regions under the condition that the liquid water path was the same.

The second AIE was first proposed by Albrecht (1989). He showed that a higher t N_d and a smaller droplet size could inhibit or slow down precipitation formation, and thereby increase the cloud liquid water path (LWP) and cloud lifetime. However, the second AIE is inextricably entangled with the meteorological background, other physical processes and feedbacks (e.g., turbulence [cloud entrainment/detrainment]) (Ackerman et al. 2003; Ackerman et al. 2004), and even surface fluxes. Therefore, the second AIE is extremely difficult to quantify (Penner et al. 2001).

The study of the AIE in maritime clouds has attracted considerable attention in recent years. Maritime clouds occur frequently, and cover a large area and have a relatively high albedo (about 0.3-0.4) compared to the underlying ocean surface (about 0.1) (Randall et al. 1984). By investigating three nocturnal maritime stratocumulus cloud cases, Ackerman et al. (2004) pointed out that the LWP increased with N_d for the range of N_d they considered (~25-350 cm^{-3}), only if the atmosphere above the cloud layer was moist (the relative humidity reached at least 70%) or there was significant precipitation at the surface (specifically, the average surface precipitation rate exceeded 0.1 mm/day). Otherwise, the cloud water content might decrease as N_d increased because of the enhanced entrainment of the dry air at the cloud top. Entrainment was enhanced when N_d increased because the net condensational heating by the formation of precipitation/drizzle was reduced. Condensational heating reduces the radiative cooling at cloud top and results in a sharp decrease of entrainment at the cloud top (Stevens et al. 1998).

Lu and Seinfeld (2005) examined an ensemble of 98 three-dimensional ERM simulations of marine stratocumulus clouds to explore the AIE. They conducted a statistical analysis and showed that the cloud LWP responded primarily to the large-scale subsidence and sea surface temperature. The cloud LWP tended to be positively correlated with N_a when there was heavy surface precipitation, otherwise it did not. This positive (non-positive) correlation would enhance (reduce) the overall AIE for the heavily (lightly) drizzling clouds.

Are these results also applicable to continental clouds? It is surprising that continental clouds have not received the same scrutiny as marine clouds, even though most global climate models suggest that the total AIE over land should be at least as large as that over oceans (Lohmann & Feichter 2005). The continental boundary layer differs from the marine boundary layer because the surface sensible and latent heat fluxes vary significantly over the diurnal cycle (Garstang & Fitzjarrald 1999). The continental boundary layer grows rapidly after sunrise and reaches its maximum (1 km or more) just before sunset. At night, it decreases dramatically to only a couple of hundred meters thick. In contrast, the depth of the marine boundary is far more constant, and undergoes only a weak diurnal cycle. It often becomes slightly deeper at night because of radiative cooling.

Han et al. (2002) used satellite data to examine the global cloud liquid water path sensitivity (δ) to cloud droplet number concentration during the daytime, specifically in the local afternoon from 14:00 Local Standard Time (LST) to 16:00 LST. (δ is defined as the ratio of the change of cloud LWP to the change of column-integrated cloud droplet number concentration (N_c), that is, $\delta = \frac{\Delta LWP}{\Delta N_c}$). They analyzed δ over oceans and over land. According to their analysis, marine clouds have areas with both large positive and large negative δ, and these areas have a strong seasonal dependence; (i.e., negative δ tends to occur over the summer hemisphere ocean). For most continental clouds, δ is neutral or slightly negative. This may mean that an increase of N_a, and therefore, N_c, does not necessarily result in an increase of cloud LWP, which could imply a negligible or even negative second AIE (Albrecht 1989).

Since the second AIE involves dynamic, radiative, and surface flux feedbacks in the response of the cloud water and its vertical and horizontal extent to aerosol loading, there may be some other factors or feedbacks that operate in the continental environment and play a role in the response of clouds to N_a. For example, Ovtchinnikov and Ghan (2005) stressed the dominant effect of the dynamical framework on both the microphysical and the macrophysical properties of their simulated continental cloud, and they pointed out that this effect was much stronger than the AIE.

To advance our scientific understanding of aerosol-cloud-radiation interaction, the U.S. Department of Energy's Atmospheric Radiation Measurement (ARM) Program conducted an Aerosol Intensive Operation Period at its Southern Great Plains site in May 2003 (Ferrare et al. 2006; Feingold et al. 2006). During this Aerosol Intensive Operation Period, measurements of the cloud condensation nucleus concentration as a function of supersaturation were taken to relate cloud condensation nucleus concentration to aerosol composition and size distribution. Airborne measurements of the cloud droplet number concentration were also made. Because the field campaigns were limited in time and space, remote-sensing techniques also were intensively employed at the Southern Great Plains site to provide cloud microphysical, macrophysical, and radiative properties. These techniques provided droplet effective radius, cloud morphology and cloud optical depth, which provided a good opportunity to study the role of aerosols in continental large-scale clouds.

In this study, we use a cloud resolving model (i.e., the Active Tracer High-resolution Atmospheric Model [ATHAM]) to discuss the effect of aerosol loading on the cloud droplet effective radius (R_e), and on the cloud LWP. The case we examine is a stratiform cloud that occurred on May 17, 2003. Sensitivity tests are conducted to investigate the AIE and the impact of the surface energy and moisture fluxes on the cloud development.

The paper is organized as follows: The Model Description and Simulation Setup section describes ATHAM and the simulation set-up. The Sensitivity Tests section presents a series of sensitivity tests. The Conclusions and Discussion section discusses and summarizes our results.

Model Description and Simulation Setup

Model Description

ATHAM is a non-hydrostatic, compressible atmospheric model that solves the Navier-Stokes equations and is formulated with an implicit-time step and a finite-difference scheme (Oberhuber et al. 1998; Herzog 1998; Herzog et al. 1998; Herzog et al. 2003; Guo et al. 2004, 2005). The model predicts momentum, potential temperature, pressure, turbulent kinetic energy, turbulent length scale, and tracers (e.g., specific humidity, cloud water, rain water, ice, and graupel). To have better conservation properties, the model solves momentum equations, tracer equations, and the thermodynamic equation in the flux form, rather than the adjective form. As is customary for cloud resolving models, it applies a

periodic lateral boundary condition. At the lower boundary, it assumes a material surface, across which surface sensible heat and moisture fluxes pass. The model top is a rigid lid. At the upper part of the numerical domain (upper 20%), a sponge layer is applied to minimize the spurious reflection of upward propagating gravity waves.

Simulation Set-Up

ATHAM can be set up by using either a two-dimensional or three-dimensional framework. The two-dimensional framework has been employed in this study. Three-dimensional simulations were also performed for our base case. The simulated cloud microphysical and macrophysical properties for the three-dimensional simulation are similar to those for the two-dimensional results, and are evaluated well against observations. Grabowski et al. (1998) also demonstrated that two-dimensional simulations could be used as realizations of cloud systems. In the following, for computational efficiency, we focus on our two-dimensional simulations. It is expected that two-dimensional results might differ from the three-dimensional counterpart quantitatively, but not qualitatively.

In this study, we use a horizontal domain of 210 km with a uniform grid resolution of 2 km. The vertical domain is 20 km and uses a stretched grid, which is uniformly 40 m for the lowest 2 km and then relaxed to about 300 m near the model top. The time step is about 3 seconds.

Sensitivity Tests

Sensitivity to Aerosol Particle Number Concentration

In this section, we will artificially increase (double) and decrease (halve) the aerosol number concentration (N_a) to examine both the first and the second AIE. From observations, the total N_a is about 1200 cm^{-3}, which is referred as "N_a1200" (base case). In the sensitivity test "N_a2400," N_a is doubled in each aerosol size bin (Figure 1); (i.e., the total N_a is about 2400 cm^{-3}). In the sensitivity test "N_a600," N_a is reduced to half of the base case value in each aerosol size bin. Two additional sensitivity tests are also examined where the total N_a is reduced again to 300 cm^{-3} and again to 150 cm^{-3}, i.e., "N_a300" and "N_a150," respectively (Figure 1 and Table 1). In these four sensitivity tests, the model set-ups are the same as those in the base case ("N_a1200") except for N_a.

Figures 2 and 3 show the temporal evolution of the spatial averages of N_d, R_e, drizzle rate at cloud base, and cloud LWP in the four sensitivity tests and in the base case. With increased N_a, the total N_d consistently increases and R_e consistently decreases. N_d also exhibits a diurnal variation. In the morning, it reaches its maximum and reaches its minimum in the afternoon. Table 1 presents the domain and time-averaged N_d and R_e. Most of the aerosol particles (around 70%) are activated to form cloud drops, especially in the case of low N_a. This is because most of the measured aerosol particles are in the accumulation mode and can readily be nucleated if supersaturations are high enough (the lower

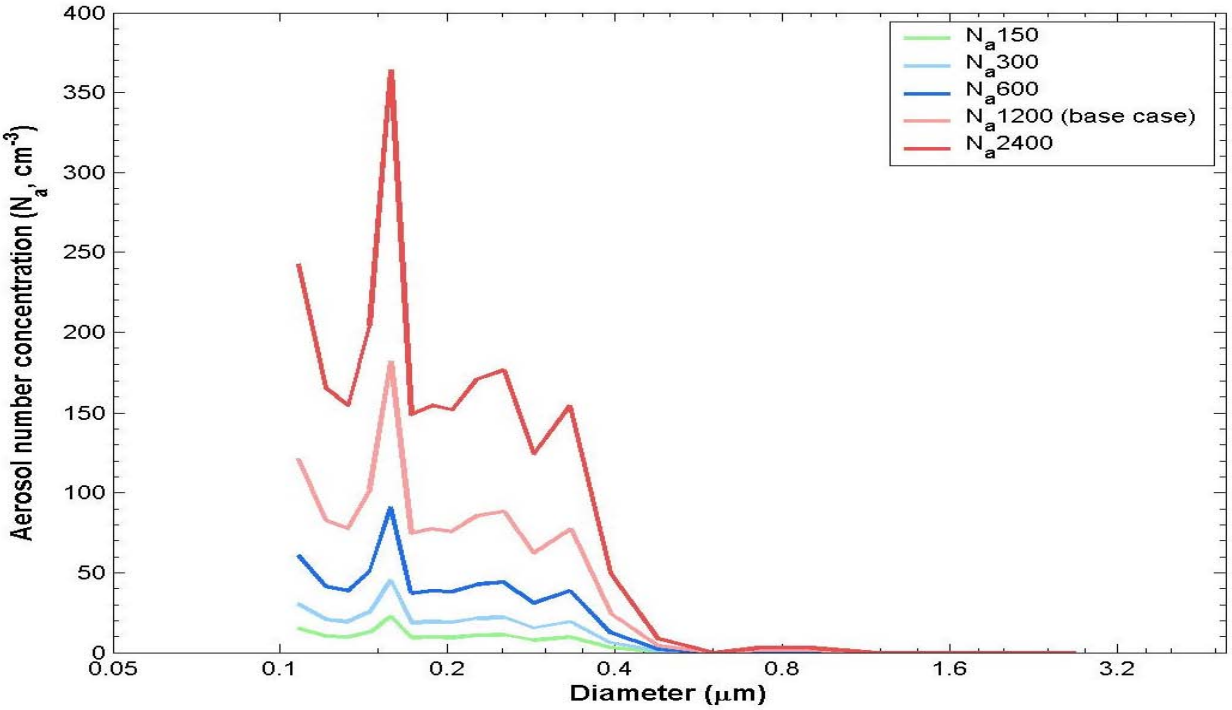

Figure 1. The aerosol particle size distribution from the Passive Cavity Aerosol Spectrometer measurement, which is used in the base case (solid line, "N_a1200"). Other distributions are used in 4 sensitivity tests of N_a150—N_a2400 (as shown in Table 1).

Table 1. Results from the sensitivity tests for increasing and decreasing N_a

Name	Total N_a (/cm^3)	Total N_d (/cm^3)	R_e (μm)	N_a (g/m^2)	Drizzle (mm/day)
Na150	150	114	9.44	74.64	0.552
Na300	300	224	7.79	83.56	0.372
Na600	600	451	6.49	99.83	0.161
Na1200 (base case)	1200	853	5.29	110.74	0.018
Na2400	2400	1,374	4.53	110.93	0.004

LWP and R_e are the spatial and temporal average.

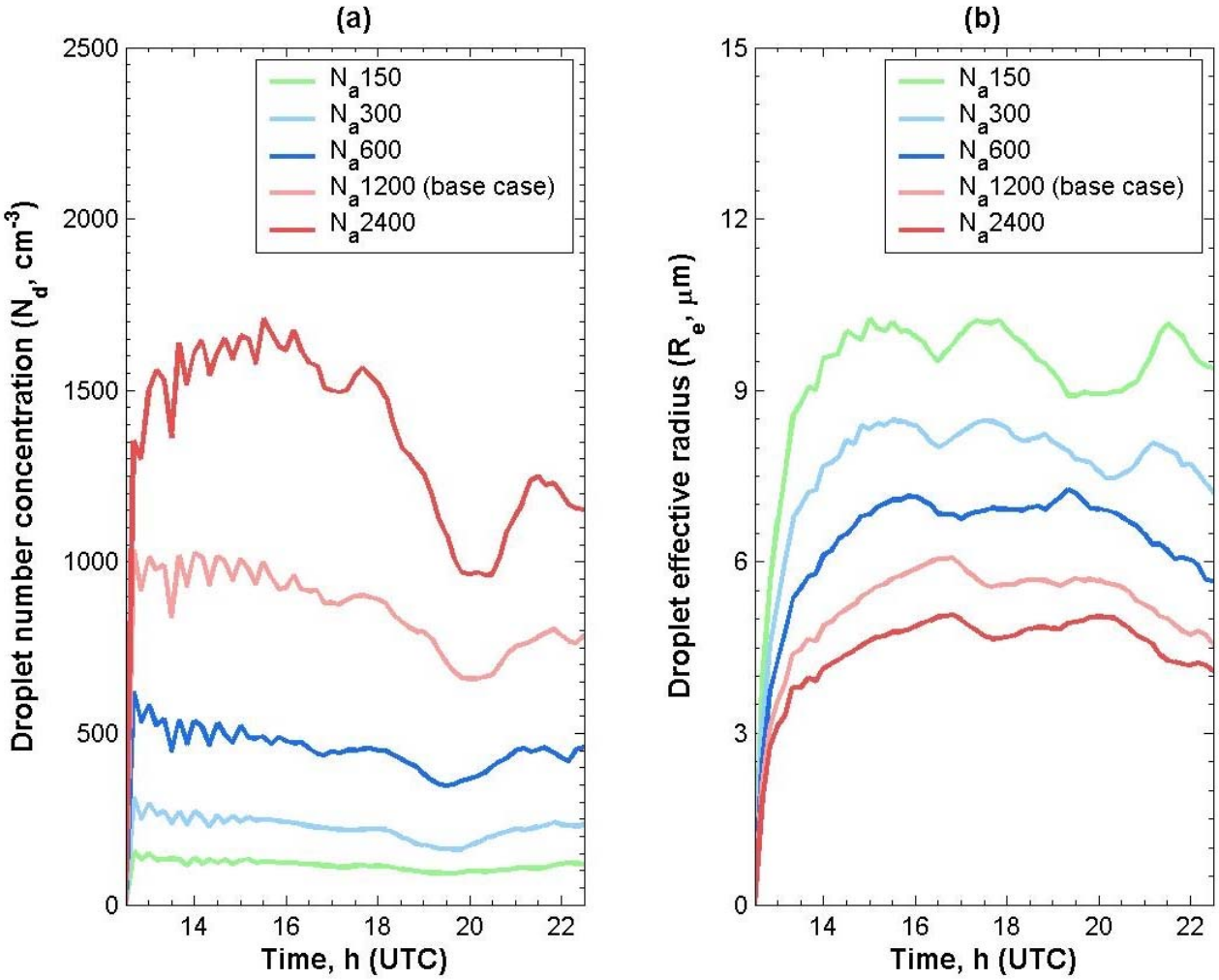

Figure 2. Time series of the spatially averaged (a) cloud droplet number concentration (N_a), and (b) effective radius (R_e) within the cloud layers in the base case and in 4 sensitivity tests (line types are indicated in the legend).

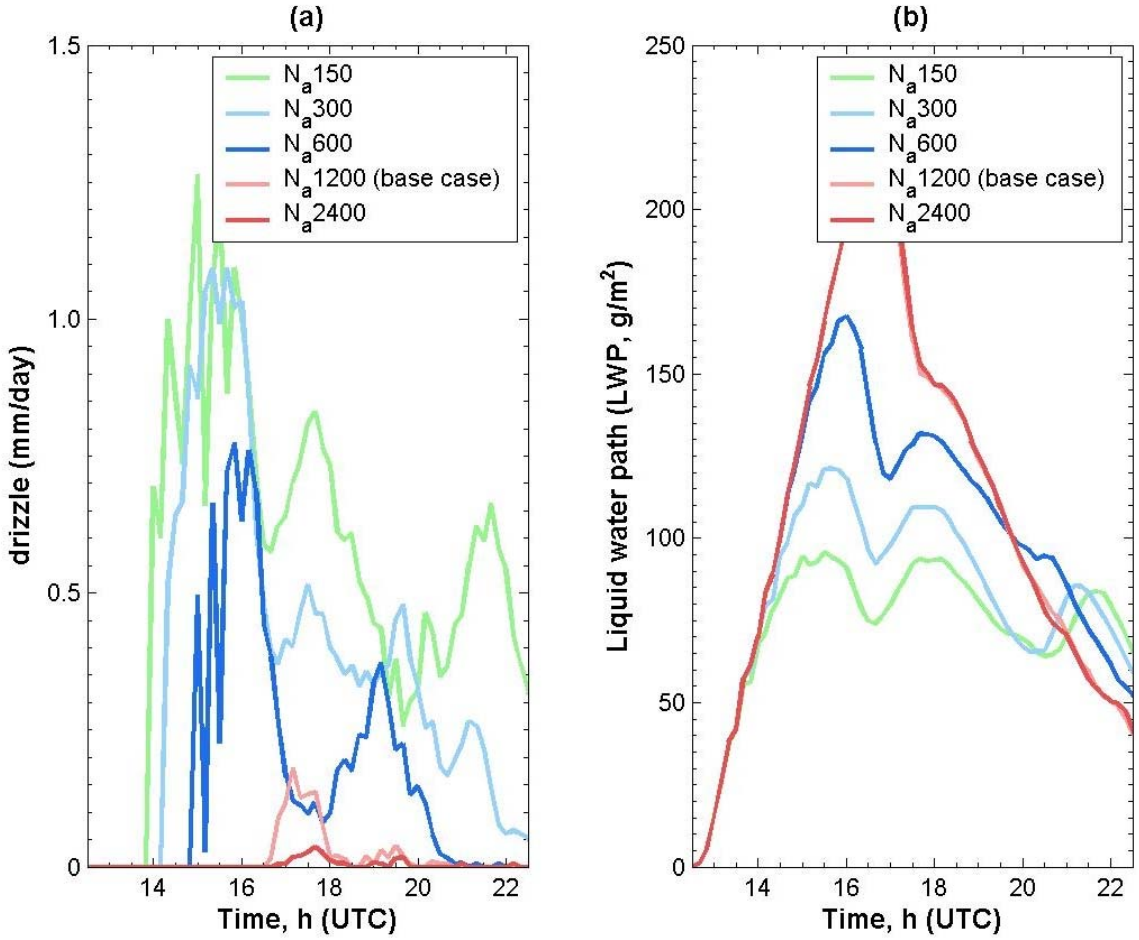

Figure 3. The same as in Figure 2, but for (a) the drizzle rate below the cloud base, and (b) the cloud LWP (Note: in the base case of "N_a1200" and the sensitivity test of "N_a2400," the cloud LWPs are almost the same so that the two curves overlap).

size limit of the Passive Cavity Aerosol Spectrometer measurement is 0.1 μ m in diameter). With N_a lower than the base case ("N_a150," "N_a300," and "N_a300"), a slightly larger fraction (≈75%) of the aerosol particles are nucleated. With N_a higher than the base case ("N_a2400"), relatively fewer aerosol particles (≈57%) are activated.

The cloud LWC can be related to N_d and R_e by $LWC = \frac{4}{3}\pi(R_e/\beta)^3 N_d$ (Note: we assume that R_ε is linearly proportional to the volume-mean radius R_v, that is, $R_e = \beta R_v$, where β is 1.143 for the continental clouds [Martin et al. 1994; Lohmann et al. 1999]). For a given cloud LWC, R_e is inversely proportional to $N_d^{1/3}$. If N_d is doubled, R_e will be reduced by 20%, theoretically. From Table 1, we can find that R_e is reduced by 17% when N_a is doubled. This is because the cloud LWC increases with higher N_a in the relatively clean scenarios ("N_a150," "N_a300," and "N_a600"). In addition, fewer aerosol particles are activated in the polluted scenarios ("N_a1200" and "N_a2400").

The time evolution of N_d and R_e (Figure 2) and the time averages of N_d and R_e (Table 1) for the sensitivity tests show that the first AIE is evident and robust. However, the second AIE is not as striking as the first AIE (Figure 3 and Table 1). When N_a is increased from 1200 cm^{-3} to 2400 cm^{-3} (i.e., "N_a1200" and "N_a2400"), the domain and time averaged cloud LWP is almost unchanged (from 110.74 $g/m^2$to 110.93 g/m^2), although there is about a 10% decrease of the cloud LWP when N_a is reduced by half and this decrease continues when N_a is reduced further (Table 1). Note that the drizzle rate below the cloud base generally decreases as N_a increases. However, when the precipitation is reduced to a negligible amount, further increases in N_a do not contribute to allowing clouds to contain more cloud water, and the response of the cloud LWP to increases in N_a (due to the lack of precipitation) becomes insignificant. Thus, an increase of N_a *does* not necessarily lead to an increase of cloud LWP (comparing "N_a1200" and "N_a2400"). Only when there is significant precipitation, does cloud LWP increase with N_a, as in the cases with N_a equal to 150, 300, 600 and 1200 cm^{-3}.

As shown in Figure 3, the differences in the cloud LWP among the four sensitivity tests are only distinguishable after five or six hours of simulation time when the precipitation forms in the base case, which is similar to the continental cloud case studied by Ovtchinnikov and Ghan (2005). The cloud LWP increases (or at least does not decrease) with N_a during the first part of the simulation (before 20:00 Universal Time Coordinates [UTC]). However, it decreases with N_a after 20:00 UTC. The cloud LWP in the cleanest case ("Na150") becomes the highest among the four sensitivity tests and base case after 21:30 UTC, which is just opposite to the second AIE hypothesis. This result is associated with drizzle evaporative cooling. Figure 4a shows the time evolution of the column-integrated evaporation rate by the falling drizzle. Obviously, "N_a150" has the strongest drizzle evaporation rate because of the highest drizzle production among the five simulations (four sensitivity tests and one base case). The vertical profiles of the evaporative cooling rate averaged over the last 2 hours (from 20:30 UTC to 22:30 UTC) are presented in Figure 4b. Within the sub-cloud layers and cloud base (from 300 m to about 1000 m), there is a significant evaporative cooling which can reach up to 0.18 K/h for the "N_a150"case. Therefore, "N_a150" would be expected to have the coldest sub-cloud layer among the five simulations.

Figure 5a shows the difference in the horizontally and temporally averaged temperature profiles from 20:30 UTC to 22:30 UTC between the base case ("N_a1200") and three sensitivity tests for "N_a150," "N_a300" and "N_a600." (Note the temperature and moisture profiles for the sensitivity test for "N_a2400" are almost identical to those of the base case "N_a1200" and are therefore omitted.) The temperatures at cloud base in the sensitivity tests for "N_a150," "N_a300," and "N_a600" are lower than that in the base case ("N_a1200") by 0.25, 0.2, and 0.1 K on the average, respectively (Figure 5a). Less water vapor can be held at these colder temperatures and therefore more water vapor condenses to form cloud water. The horizontally and temporally averaged specific humidity at cloud base in the tests for "N_a150," "N_a300," and "N_a600" are smaller than those in the base case by 0.15 g/Kg, 0.12 g/Kg, and 0.07 g/Kg, respectively (Figure 5b). However, the horizontally and temporally averaged cloud LWCs are larger by 0.11 g/Kg, 0.10 g/Kg, and 0.08 g/Kg, respectively (Figure 5c). We note that the temperature and the

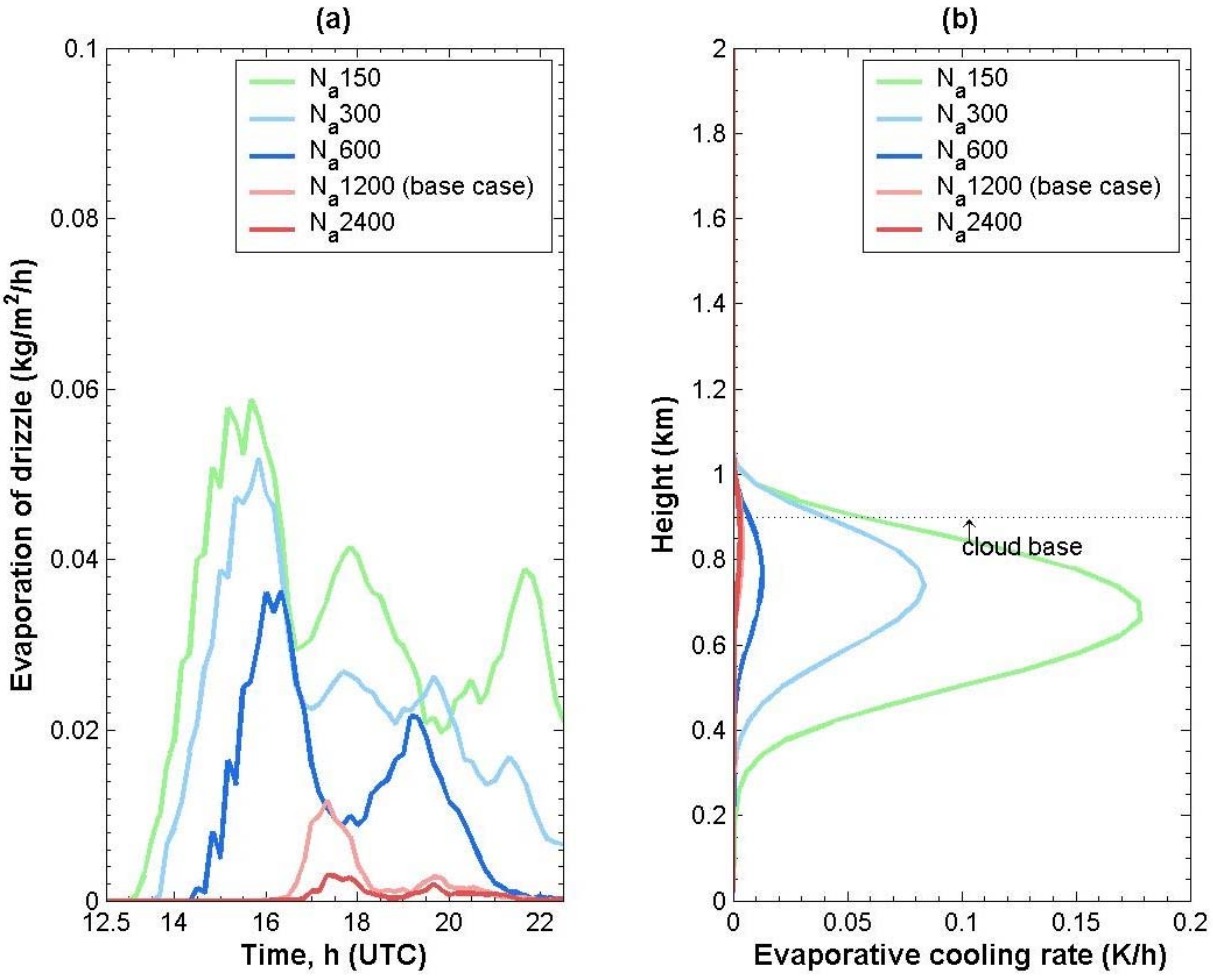

Figure 4. Time series of the horizontally averaged (a) column-integrated drizzle evaporative rate, and (b) profiles of drizzle evaporative cooling rate averaged over the last 2 hours of the 11-hour simulation for the base case (N_a1200) and for the 4 sensitivity tests (N_a150---N_a2400) (line types are indicated in the legend).

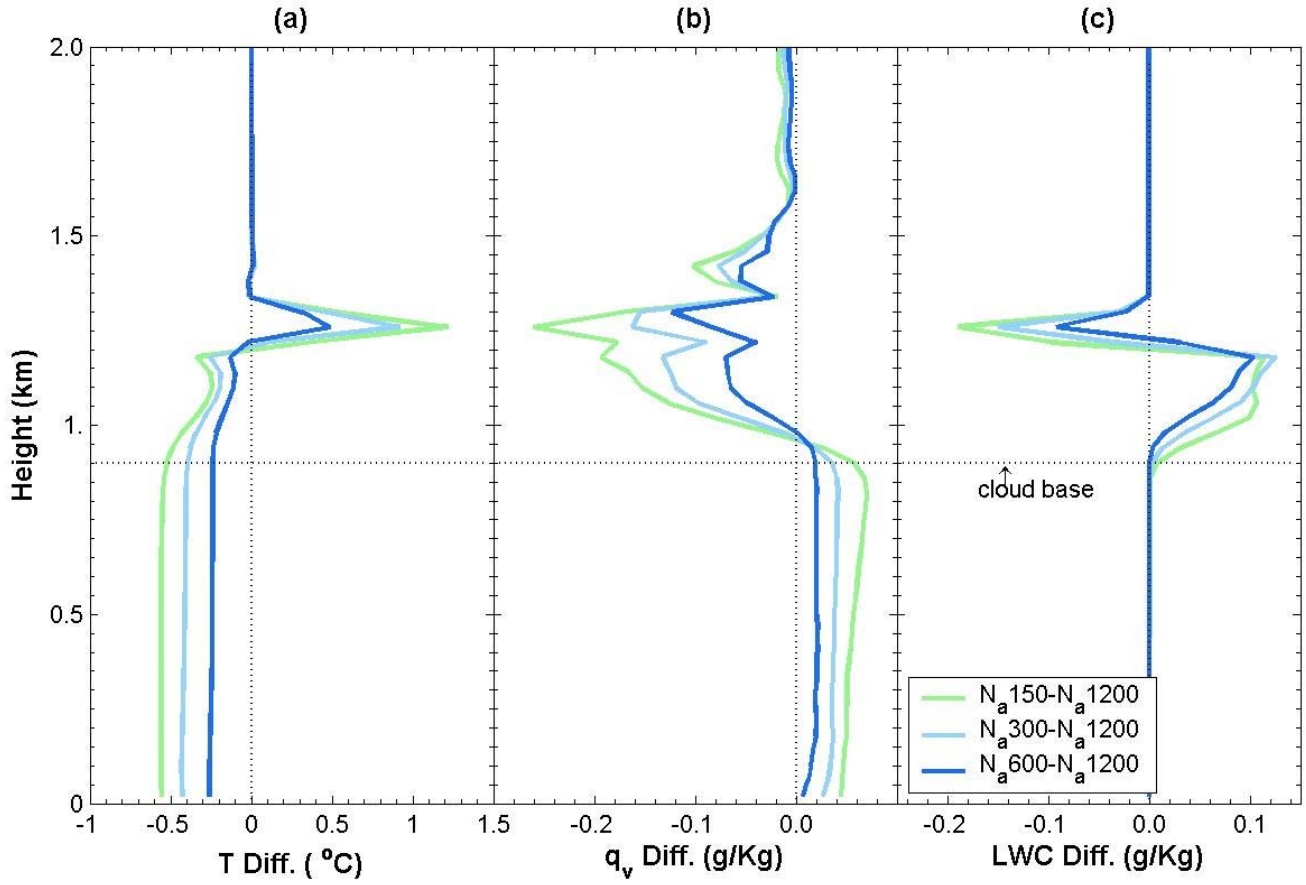

Figure 5. The vertical profiles of the difference in the horizontally averaged (a) in-situ temperature, (b) specific humidity and (c) cloud liquid water content, averaged over the last 2 hours of the 11-hour simulation, between the sensitivity test "N_a600" and the base case "N_a1200" (solid), between the sensitivity test "N_a300" and the base case "N_a1200" (dashed), and between the sensitivity test "N_a150" and the base case of "N_a1200" (dotted).

specific humidity at the cloud top are higher in the tests for N_a150, N_a300, and N_a600 than those in the base case, while the cloud LWC is lower. Since the cloud LWP is the vertical integral of the cloud LWC over the cloud layers, the cloud LWP is determined by both the cloud geometrical thickness (H) and the cloud LWC vertical distribution. The vertical extent of the layers with decreased LWC at cloud top is smaller than the vertical extent of the layers with increased LWC near cloud base. The cloud LWP is therefore dominated by the contribution from the lower part of the cloud here. As a result, the cloud LWP tends to become larger with smaller N_a. Feingold et al. (1996) showed that when only a small amount of drizzle was produced in a cloud, the evaporative cooling tended to be just below cloud base and resulted in a destabilization and a more vigorous circulation. They further hypothesized that this destabilization could enhance cloud liquid water.

Sensitivity Tests for Surface Latent and Sensible Heat Fluxes

As discussed in the Sensitivity to Aerosol Particle Number Concentration section, the cloud LWC depends on the thermodynamic vertical profile. With the same moisture profile, the cloud LWC will be higher in a cooler atmosphere (e.g., Figure 5). Given the same vertical temperature profile, the cloud LWC can also be higher if there is a larger moisture supply. In this section, we will explore the impact of the surface latent and sensible heat fluxes on the cloud morphology and cloud evolution.

First, we examine the effect of the surface latent heat flux by increasing and decreasing it by 25%, referred as "N_a1200_1.25LHFlx" and "N_a1200_0.75LHFlx." As expected, a larger surface latent heat flux leads to a higher cloud LWP, and vice versa (Figure 6). The spatial and temporal average of the cloud LWP increases and decreases by 7% in the "N_a1200_1.25LHFlx" case and in the "N_a1200_0.75LHFlx" case, respectively, compared to the base case "N_a1200" (Table 2). In both "N_a1200_1.25LHFlx" and "N_a1200_0.75LHFlx," there is little precipitation (not shown here). Therefore, an important cloud water sink is not present, and there is no feedback from evaporative cooling as discussed above. The surface moisture flux is effectively transported upward and reaches the cloud layers in this well-mixed boundary layer. As a result, the cloud LWP responds almost linearly to the enhanced (reduced) surface moisture supply.

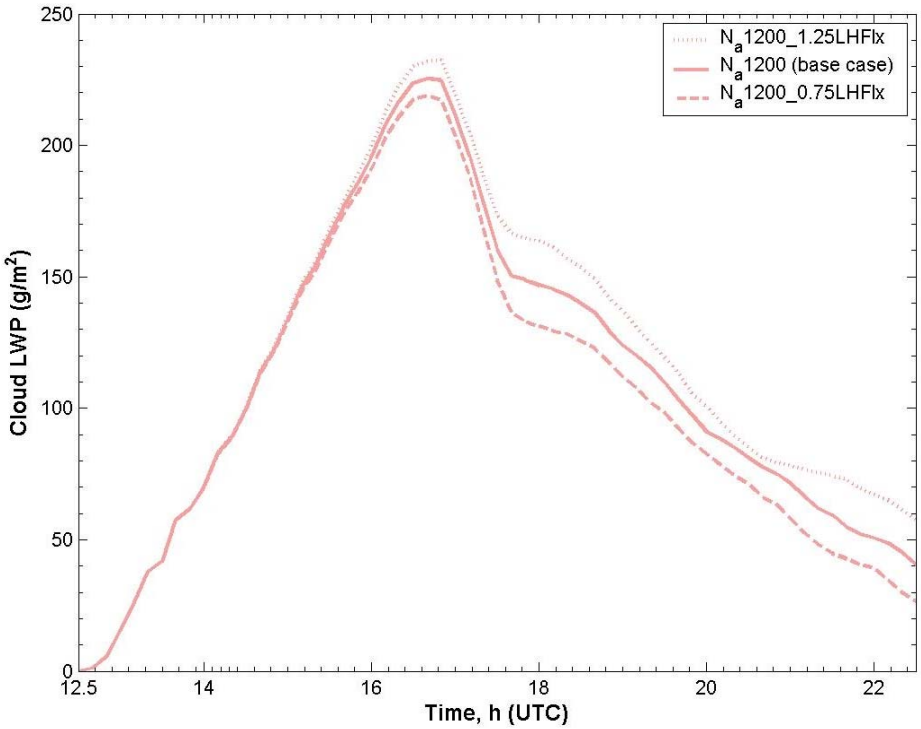

Figure 6. Time series of the horizontally averaged cloud LWP in the base case (solid), and in the sensitivity tests increasing (dotted) and decreasing (dashed) the surface latent heat flux by 25%.

Table 2. Results from the sensitivity tests for increasing and decreasing surface sensible and latent heat fluxes.

Name	Surface fluxes		(in-cloud) LWP (g/m^2)	R_e (μm)	$\overline{H}$ (m)	$\overline{CLWC}$ (g/m^3)
	sensible	latent				
Na1200_1.25LHFlx	×1.	×1. 25	116.92	5.28	302.32	0.36
Na1200_0.75LHFlx	×1.	×0.75	101.83	5.07	281.33	0.33
Na1200_1.25SHFlx	×1.25	×1.	86.57	4.84	266.91	0.29
Na1200_0.75SHFlx	×0.75	×1.	116.97	5.47	350.19	0.33
Na1200 (base case)	×1.	×1.	110.74	5.29	293.14	0.34

Table 2 presents the horizontal and temporal average of the cloud geometrical thickness ($\overline{H}$) and the spatial and temporal average of the cloud LWC ($\overline{CLWC}$). Both $\overline{H}$ and $\overline{CLWC}$ increase/decrease almost linearly (by 3-4%) in response to the increase/decrease of the surface latent heat flux (by 25%). Thus, a higher surface moisture supply can not only promote the cloud moisture, but also deepen the cloud layer.

Over land, the surface sensible heat flux undergoes a large diurnal variation as land surfaces respond faster to the solar forcing. The planetary boundary layer (PBL) begins to grow a half hour after sunrise and the maximum PBL depth occurs near sunset. The PBL is often characterized by an intense mixing of warm air rising from the surface. However, as the night progresses, the PBL usually collapses to a shallow layer (Stull 1988; Medeiros et al. 2005). Two sensitivity tests for increasing and decreasing the surface sensible heat flux by 25% were also carried out (denoted as "N_a1200_1.25SHFlx" and "N_a1200_0.75SHFlx," respectively). Figure 7 shows the temporal evolution of the horizontally averaged in-cloud LWP and cloud fraction. An enhanced surface sensible heat flux helps "evaporate" clouds and leads to a reduction of both the in-cloud LWP and the cloud fraction. Figure 8 shows the temporal evolution of the cloud LWC for "N_a1200_1.25SHFlx" and "N_a1200_0.75SHFlx."

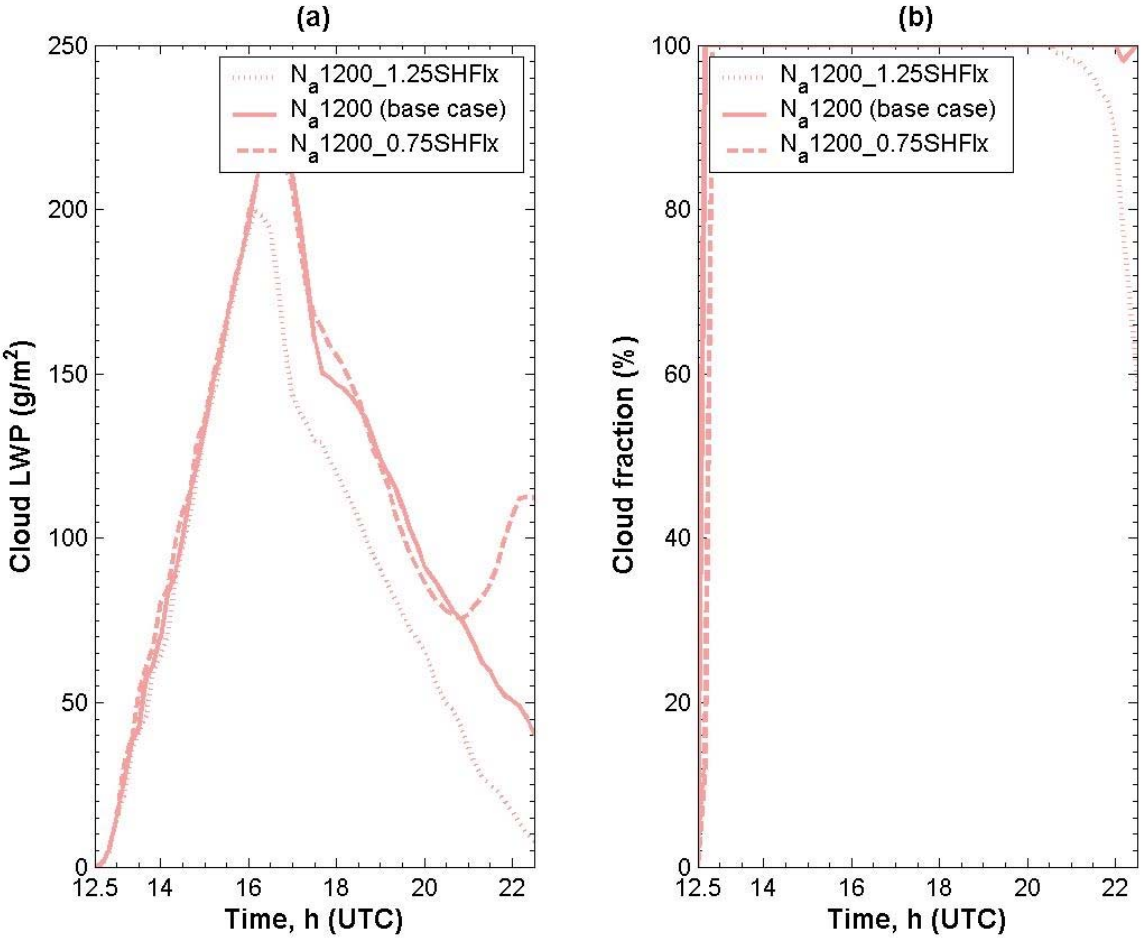

Figure 7. Time series of the horizontally averaged in-cloud LWP and cloud fraction in the base case (solid), and in the sensitivity tests with increasing (dotted) and decreasing (dashed) the surface sensible heat flux by 25%.

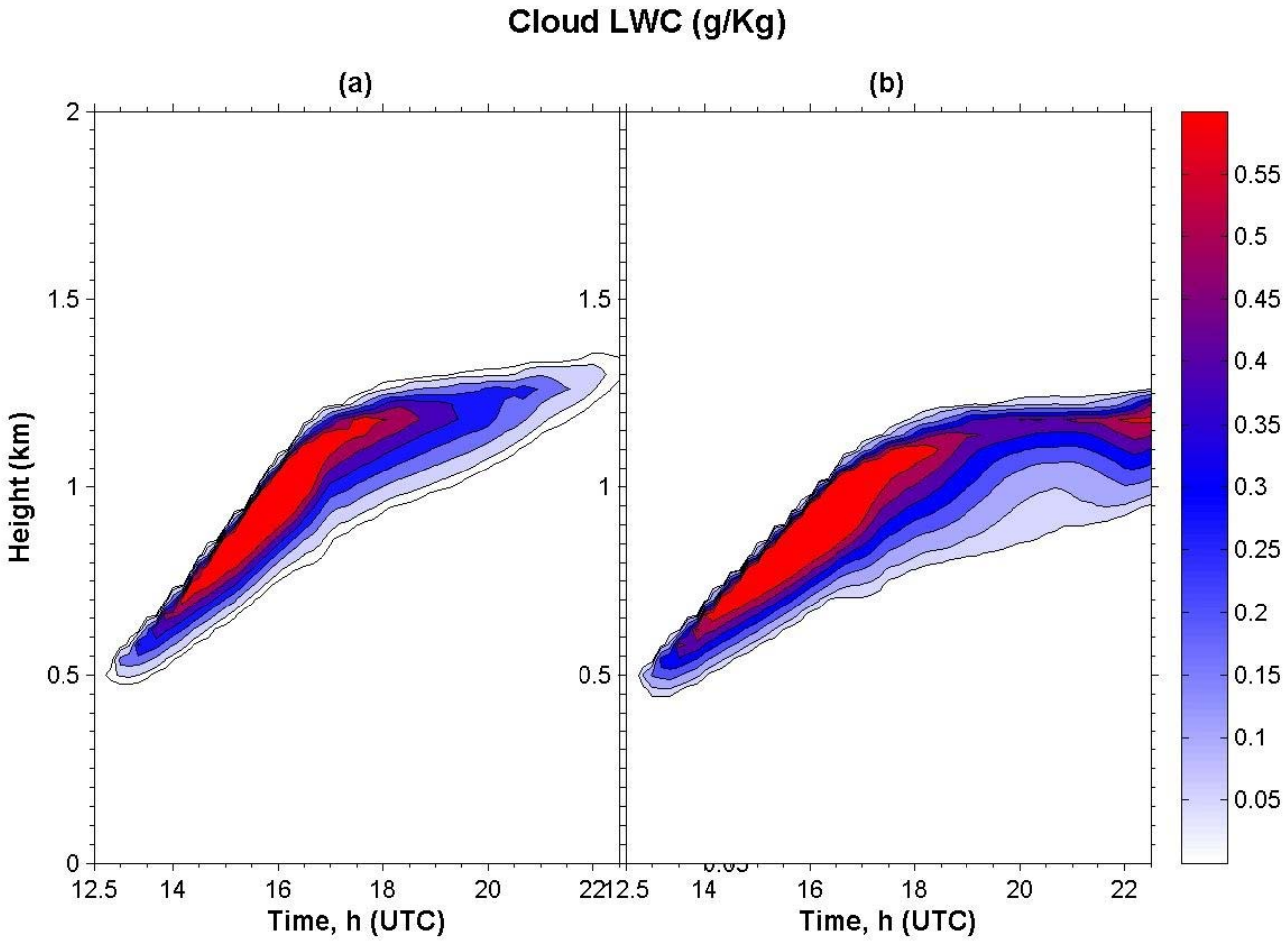

Figure 8. Time-height cross section of horizontally averaged cloud LWC in the sensitivity tests with increasing (left panel) and decreasing (right panel) surface the sensible heat flux by 25%.

From 12:30 UTC to 20:00 UTC, the magnitudes of the cloud LWC and their spatial distributions in these two tests are similar. However, the cloud tends to become shallower in "N_a1200_1.25SHFlx." Both the cloud top and cloud base rise faster in "N_a1200_1.25SHFlx" than those in "N_a1200_0.75SHFlx" (Figure 9). From 13:00 UTC to 20:00 UTC the cloud base rises from 0.5 km to 1.0 km and cloud top rises from 0.5 km to 1.3 km in "N_a1200_1.25SHFlx." (Note: the cloud base and top in ATHAM are defined as the lowest and highest model levels with the cloud LWC > 0.001g/Kg and $N_d > 5/cm^3$). However, over the same period in "N_a1200_0.75SHFlx," the cloud base rises from 0.5 km to 0.8 km and cloud top rises from 0.5 km to 1.3 km. The difference in the cloud tops between "N_a1200_1.25SHFlx" and "N_a1200_0.75SHFlx" is much less pronounced than the difference in the cloud bases. The cloud base is higher and the cloud is shallower in "N_a1200_1.25SHFlx." A higher surface sensible flux causes a deeper sub-cloud layer (i.e., an enhanced cloud base), and results in a lower cloud LWP (Golaz et al. 2001). As shown in Table 2, $\overline{CLWC}$ is reduced by only 10% from

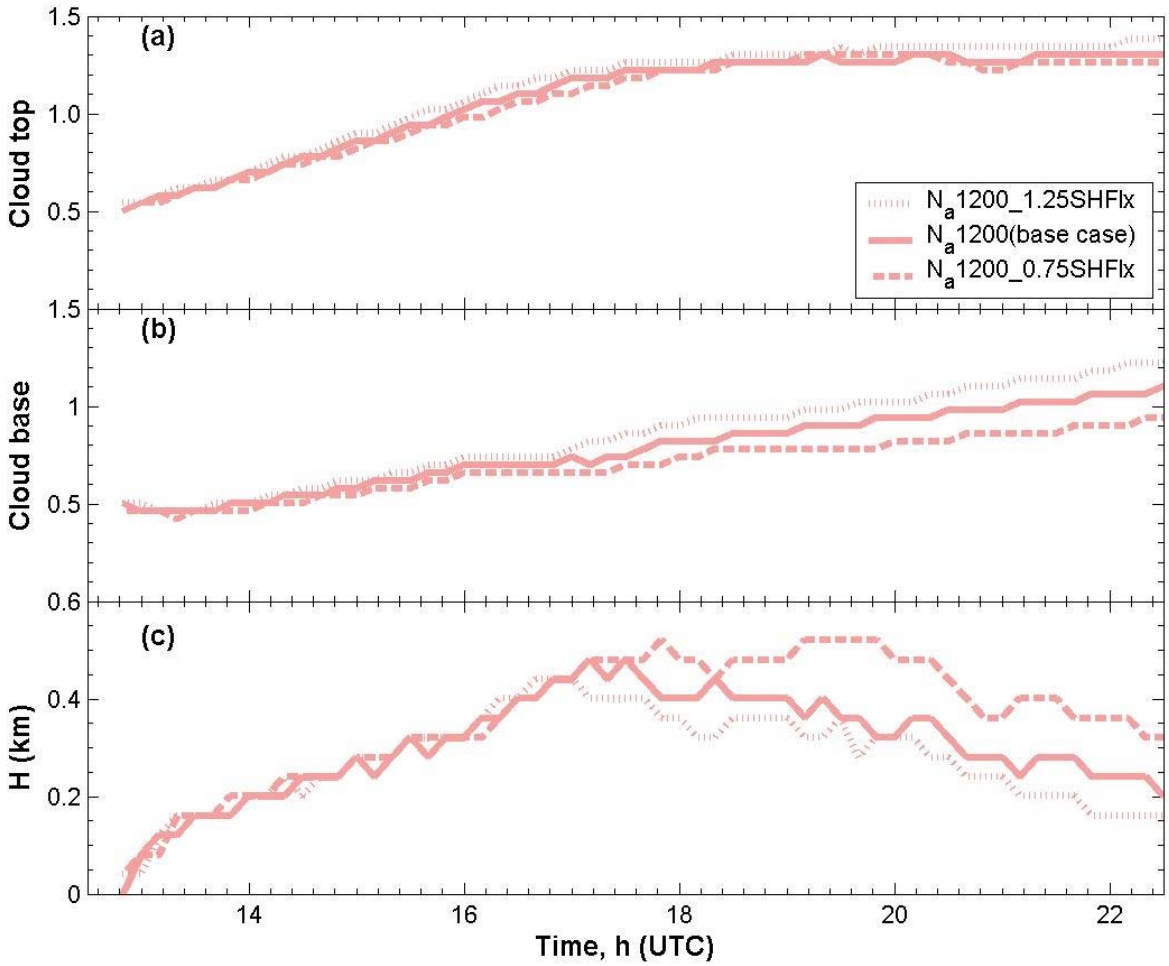

Figure 9. Time series of the horizontally averaged heights of (a) cloud base, (b) cloud top, and (c) cloud geometrical thickness (*H*) in the base case (solid line), and in the sensitivity tests with increasing (dotted) and decreasing (dashed) the surface sensible heat flux by 25%.

"N_a1200_0.75SHFlx" to "N_a1200_1.25SHFlx." However, $\overline{H}$ is reduced by 24%, and the in-cloud LWP is reduced by 27%. This indicates that the change of LWP is mainly attributed to the change of the cloud geometrical thickness *H* when the surface sensible heat flux changes.

On the average, the in-cloud LWP decreases from 109.67 g/m^2 to 86.57 g/m^2 (by 20%) after increasing the surface sensible heat flux by 25%; but it increases from 109.67 g/m^2 to 116.97 g/m^2 (by 7%) after increasing the latent heat flux by 25%. The cloud LWP does not respond linearly to the surface sensible heat flux, whereas it does response almost linearly to the surface latent heat flux. Surface sensible heat could influence the thermal structure of the PBL, and thereby the cloud morphology (mainly the height of cloud base). The decreased amount of cloud LWP caused by an enhancement of the surface sensible

heat flux by 25% is similar to that caused by quadrupling N_a (Tables 1 and 2). The response of cloud LWP to the change of the thermal-dynamic vertical structure is even more striking than its response to the aerosol burden.

Conclusions and Discussion

In this continental cloud that we studied, an enhancement of N_a generally resulted in a higher N_d and a smaller droplet size. The first AIE is evident and robust. However, the cloud LWP *does not always* increase with N_a. In the heavily polluted scenario where the precipitation efficiency is already very low (or negligible), an increase in N_a will not change cloud water content or cloud geometrical thickness. We show that near the end of our simulation (from 20:00 UTC to 22:30 UTC, or 14:00 LST to 16:30 LST), if there is a small amount of drizzle, the evaporation of drizzle cools the cloud base, and this cooling increases the cloud water content in the lowest layers of the cloud and results in an increase in cloud LWP when aerosol and droplet concentrations decrease. The local time for this result corresponds to that of the satellite overpass time (i.e., from 14:00 LST to 16:00 LST) in the investigations reported by Han et al. (2002) and Han et al. (1994). Thus, our result is consistent with satellite observations for continental clouds of neutral or slightly negative liquid water sensitivity to aerosol burden (Han et al. 2002). So we suspect that the evaporative cooling effect by drizzle might explain the neutral or slightly negative sensitivity over land. However, our model result might be case-dependent and needs to be further explored and examined.

We also show that cloud LWP increases with N_a only when there is a significant amount of precipitation. This is because the precipitation is an important sink of cloud water for precipitating clouds and its decrease allows the cloud LWP to increase. The spatial and temporal average cloud LWP increases as N_a increases despite the small decrease at the end of our simulations.

In this case study, the sub-cloud layer is well-mixed and the surface moisture supply is effectively transported upward. As a result, the cloud LWP responds almost linearly to the change of the surface latent heat flux. Both the cloud geometrical thickness and cloud water content increases nearly linearly with a stronger surface latent heat flux.

Variations in the surface sensible heat flux play an important role in the PBL. The surface sensible heat flux affects the depth of the PBL, and therefore determines the increase in the cloud base over time. Sensitivity tests show that the cloud base is lifted to a higher altitude given a higher sensible heat flux. As a result, the cloud tends to be thinner and drier. The impact of the surface sensible heat flux on the cloud morphology is more pronounced than its impact on the cloud water content. Therefore, the variation in the cloud LWP is largely attributable to the change of cloud geometrical thickness. Therefore, in addition to the cloud water content, cloud morphology (or cloud geometrical thickness) is also of significance in determining the cloud LWP. The decrease of cloud LWP after increasing sensible heat flux by 25% is comparable to the change after quadrupling N_a. Another consequence of the higher surface sensible heat flux is a decrease in the cloud fraction. After increasing the sensible

flux by 25%, the uniform cloud deck is broken up as a result of the lower ambient relative humidity. There is a systematic trend between the high relative humidity and the cloud water content, and their individual spatial patterns, as well.

The response of the cloud LWP to the aerosol loading is often complicated by thermo-dynamical feedbacks (e.g., cloud top entrainment, drizzle evaporative cooling and moistening, and surface fluxes), and could sometimes even be controlled by them. Surface energy flux plays an important role in determining the cloud LWP. Anthropogenic emissions of aerosols and their precursors could attenuate the incoming solar radiation and result in a reduction of solar heating at the surface ("solar dimming"). Such a reduction may result in a smaller surface energy and moisture flux transported upward to the lower atmosphere. These two factors have two competing impacts on the cloud LWP and therefore can either amplify or diminish the total AIE. A decrease in the latent heat flux might lead to a shallower and drier cloud (smaller cloud LWP). A decrease in the sensible heat flux would result in a deeper cloud (larger cloud LWP). Because surface latent and sensible flux often co-vary with each other, and correlate with the underlying soil moisture, a fully coupled atmospheric and the land-surface model is needed to investigate the net effect of aerosols on clouds and the energy budget.

Corresponding Author

Huan Guo, hguo@umich.edu, (734) 764-0564

Acknowledgments

This work was supported by the U.S. Department of Energy ARM Program under grant #DEFG02-97-ER62370, and we also acknowledge ARM Program for providing access to its Data Archive.

References

Abdul-Razzak, H, and S Ghan. 2002. "A parameterization of aerosol activation, 3. Sectional representation." *Journal of Geophysical Research* 107:4026.

Ackerman, AS, OB Toon, DE Stevens, and JA Coakley Jr. 2003. "Enhancement of cloud cover and suppression of nocturnal drizzle in stratocumulus polluted by haze." *Geophysical Research Letter* 30(7)1381.

Ackerman, AS, MP Kirkpatrick, DE Stevens, and OB Toon. 2004. "The impact of humidity above stratiform clouds on indirect aerosol climate forcing." *Nature* 432:1014-1017.

Albrecht, BA. 1989. "Aerosols, cloud microphysics, and fractional cloudiness." *Science* 243:1227-1230.

Brenguier, J-L, H Pawlowska, L Schuller, R Preusker, J Fischer, and Y Fouquar. 2000. "Radiative properties of boundary layer clouds: Droplet effective radius versus number concentration." *Journal of Atmospheric Sciences* 57:803-821.

Feingold, G, B Stevens, WR Cotton, and AS Frisch. 1996. "The relationship between drop in-cloud residence time and drizzle production in numerically simulated stratocumulus clouds." *Journal of Atmospheric Sciences* 53(8)1108-1122.

Feingold, G, R Furrer, P Pilewskie, LA Remer, Q Min, and H Jonsson. 2006. "Aerosol indirect effect studies at Southern Great Plains during the May 2003 Intensive Operations Period." *Journal of Geophysical Research* 111(D5).

Ferrare, R, G Feingold, S Ghan, J Ogren, B Schmid, SE Schwartz, and P Sheridan. 2006. "Preface to special section: Atmospheric Radiation Measurement Program May 2003 intensive operations period examining aerosol properties and radiative influences." *Journal of Geophysical Research* 111(D5).

Garstang, M, and DR Fitzjarrald. 1999. *Observations of Surface to Atmosphere Interactions in the Tropics*, Oxford University Press.

Golaz, J-C, H Jiang, and WR Cotton. 2001. "A large-eddy simulation of cumulus clouds over land and sensitivity to soil moisture." *Atmospheric Research* 59-60, 373-392.

Grabowski, WW, X Wu, MW Moncrieff, and WD Hall. 1998. "Cloud resolving modeling of tropical systems during Phase III of GATE. PART II: Effects of resolution and the third spatial dimension." *Journal of Atmospheric Science* 55:3264-3282.

Guo, H, JE Penner, M Herzog, and X Liu. 2004. "Comparison of the vertical velocity used to calculate the cloud droplet number concentration in a cloud resolving and a global climate model." In *Proceedings of the Fourteenth Atmospheric Radiation Measurement (ARM) Program Science Team Meeting*, Albuquerque, New Mexico.

Guo, H, JE Penner, and M Herzog. 2005. "Investigation of the impact of aerosols on clouds during the May 2003 Intensive operational period at the southern great plain." Presented at the Fifteenth ARM Science Team Meeting, Daytona Beach, Florida, March.

Han, Q, W Rossow, and AA Lacis. 1994. "Near-global survey of effective droplet radii in liquid water clouds using ISCCP data." *Journal of Climate* 7:465-497.

Han, Q, W Rossow, J Zeng, and R Welch. 2002. "Three different behaviors of liquid water path of water clouds in aerosol-cloud interactions." *Journal of Atmospheric Sciences* 59:726-735.

Herzog, M. 1998. Simulation der Dynamik eines Multikomponentensystems am Beispiel vulkanischer Eruptionswolken, Ph.D. thesis, Max-Planck-Institute for Meteorology, Hamburg, Germany.

Herzog, M, H Graf, C Textor, and J Oberhuber. 1998. "The effect of phase changes of water on the development of volcanic plumes." In Report No. 270, Max-Plank Institute for Meteorology.

Herzog, M, JM Oberhuber, and HF Graf. 2003. "A prognostic turbulence scheme for the non-hydrostatic plume model." *Journal of Atmospheric Science* 60:2783-2796.

Lohmann, U, J Feichter, CC Chuang, and JE Penner. 1999. "Prediction of the number of cloud droplets in the ECHAM GCM." *Journal of Geophysical Research* 104(D8)9169-9198.

Lohmann, U, and J Feichter. 2005. "Global indirect aerosol effects: a review." *Atmospheric Chemistry and Physics* 5:715-737.

Lu, M-L, and JH Seinfeld. 2005. "Study of the aerosol indirect effect by large-eddy simulation of marine stratocumulus." *Journal of Atmospheric Science* 62:3909-3932.

Martin, GM, DW Johnson, and A Spice. 1994. "The measurement and parameterization of effective radius of droplets in warm stratocumulus clouds." *Journal of Atmospheric Science* 51(13)1823-1842.

Medeiros, B, A Hall, and B Stevens. 2005. "What controls the mean depth of the PBL." *Journal of Atmospheric Science* 62:3157-3172.

Oberhuber, J, M Herzog, H Graf, and K Schwanke. 1998. Volcanic plume simulation on large scales, In Report No. 269, Max-Plank Institute for Meteorology.

Ovtchinnikov, M, and SJ Ghan. 2005. "Parallel simulations of aerosol influence on clouds using cloud-resolving and single-column models." *Journal of Geophysical Research* 110:D15S10.

Penner, JE, M Andreae, H Annegarn, L Barrie, J Feichter, D Hegg, A Jayaraman, R Leaitch, D Murphy, J Nganga, G Pitari, and et al. 2001. "Climatic Change 2001, The Scientific Basis, Chapter 5: Aerosols, their direct and indirect effects," pp. 289-348, Cambridge University Press, 2001, ed. by JT Houghton and Y Ding and DJ Griggs and M Noguer and PJ van der Linden and X Dai and K Maskell and CA Johnson, Report to Intergovernmental Panel on Climate Change from the Scientific Assessment Working Group (WGI).

Penner, JE, X Dong, and Y Chen. 2004. "Observational evidence of a change in radiative forcing due to the indirect aerosol effect." *Nature* 427(15)231-234.

Randall, DA, JA Coakley, CW Fairall, RA Kropfli, and D Lenschow. 1984. "Outlook for research on subtropical marine stratiform clouds." *Bulletin of the American Meteorology Society* 65:1290-1301.

Stephens, GL. 2005. "Cloud feedbacks in the climate system: A critical review." *Journal of Climate*, 18:237-273.

Stevens, B, WR Cotton, G Feingold, and C-H Moeng. 1998. "Large-eddy simulations of strongly precipitating, shallow, stratocumulus-toped boundary layers." *Journal of Atmospheric Science* 55:3616-3638.

Stull, RB. 1988. "An introduction to boundary layer meteorology." Kluwer Academic Publishers, the Netherlands.

Twomey, S. 1977. "The influence of pollution on the shortwave albedo of clouds." *Journal of Atmospheric Science* 34:1149-1152.